DALTON
FULL PAPER

Dinuclear $Co^{II}M^{II}$ (M = Pb or Co) complexes having a "Co(salen)" entity in a macrocyclic framework: ligand modulation effect and neighboring metal(II) effect upon oxygenation at the "Co(salen)" center

Hideki Furutachi,*[a] Shuhei Fujinami,[a] Masatatsu Suzuki[a] and Hisashi Ōkawa *[b]

[a] *Department of Chemistry, Faculty of Science, Kanazawa University, Kakuma-machi, Kanazawa, 920-1192, Japan*
[b] *Department of Chemistry, Graduate School of Science, Kyushu University, Hakozaki, Higashi-ku, Fukuoka, 812-8581, Japan*

Received 8th March 2000, Accepted 19th June 2000
Published on the Web 21st July 2000

Dinuclear $Co^{II}Pb^{II}$ and $Co^{II}Co^{II}$ complexes, $[CoPb(L)(CH_3OH)][ClO_4]_2$ ($L^{2-} = (L^1)^{2-}$ **1** or $(L^2)^{2-}$ **2**) and $[Co_2(L)(CH_3CN)_2][ClO_4]_2$ ($L^{2-} = (L^1)^{2-}$ **3** or $(L^2)^{2-}$ **4**), have been obtained where $(L^1)^{2-}$ is a dinucleating macrocyclic ligand derived from the [2 : 1 : 1] condensation of 2,6-diformyl-4-methylphenol, ethylenediamine, and diethylenetriamine and $(L^2)^{2-}$ is an analogous ligand comprised of 1,1,2,2-tetramethylethylenediamine instead of ethylenediamine. The macrocycles have a "salen"-like N_2O_2 metal-binding site and a "saldien"-like N_3O_2 site sharing two phenolic oxygens. Crystal structures of the complexes **1**–**4** have been determined by X-ray crystallography. Complex **1** reacted reversibly with dioxygen in acetonitrile at 0 °C to form a peroxo complex $[\{CoPb(L^1)(CH_3CN)\}_2(O_2)][BPh_4]_2[ClO_4]_2\cdot 4CH_3CN\cdot 5.5H_2O$ (peroxo-**1**), whose structure was determined by X-ray crystallography. The peroxo group assumes a rare μ_3-1κ*O*,2κ*O*,3κ*O*′ binding mode, where one peroxo oxygen bridges the Co and Pb in one $\{CoPb(L^1)(CH_3CN)\}$ unit whereas the other oxygen is unidentate to the Co in another unit. Complex **3** is very sensitive to dioxygen so as to be irreversibly oxidized even at −30 °C. A $Co^{III}Co^{II}$ complex, $[Co_2(L^1)(AcO)][ClO_4]_2\cdot dmf\cdot H_2O$ (oxi-**3**), was isolated by adding sodium acetate to the oxidized solution. Complexes **2** and **4** are inert toward dioxygen.

Introduction

Bimetallic cores are versatile at the active sites of many metalloenzymes and play essential roles in biological systems by the interplay of a pair of metal ions.[1] Synthetic simple dinuclear metal complexes are important to understand the mutual influences of two metal centers on the electronic, magnetic, and electrochemical properties of such bimetallic cores.[2] Compartmental macrocyclic ligands, having two phenolic oxygens as endogenous bridge, have been developed[3–5] for this purpose, because they bind two metal centers in close proximity relevant to the active sites of bimetallic enzymes. Recent X-ray crystallographic studies have indicated that most bimetallic biosites are unsymmetric with respect to the donor atoms about the metal centers, the nature of the metal ions, the co-ordination number, and the geometric arrangement of the donor atoms.[6] Thus, the design of unsymmetric macrocyclic ligands capable of providing a discrete heterodinuclear core and unsymmetrical dinuclear core is of particular importance.[4,5] One of our objects of studying dinuclear metal complexes with unsymmetric macrocycles is to provide unsymmetrical dinuclear cores of functional significance.

The phenol-based dinucleating macrocycle $(L^1)^{2-}$, having a "salen"-like N_2O_2 metal-binding site and a "saldien"-like N_3O_2 site sharing the phenolic oxygen, was developed in our laboratory for providing discrete heterodinuclear complexes (H_2salen = *N*,*N*′-bis(salicylidene)ethylenediamine, H_2saldien = *N*,*N*″-bis(salicylidene)diethylenetriamine).[7–11] Since Co(salen) and its analogs are known for their reactivity toward dioxygen,[12,13] dinuclear $Co^{II}M^{II}$ complexes with Co^{II} in the "salen"-like N_2O_2 site of the macrocycle are of great interest for studying oxygenation at the "Co(salen)" center with respect to the participation of the metal(II) ion in the adjacent "saldien"-like N_3O_2 site.

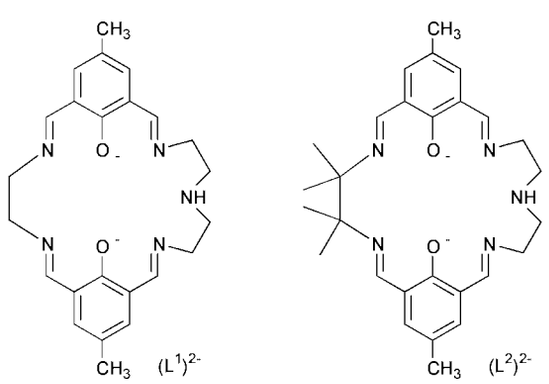

In this study the dinuclear $Co^{II}M^{II}$ (M = Pb or Co) complexes of $(L^1)^{2-}$ and analogous $(L^2)^{2-}$ having four methyl groups on the ethylene backbone have been synthesized and their crystal structures determined. They have a di(μ-phenoxo) $Co^{II}M^{II}$ core with Co^{II} in the N_2O_2 site and M^{II} in the N_3O_2 site. The M^{II} in the "saldien" site largely deviates from the mean molecular plane, providing non-equivalent *anti* and *syn* sites for axial co-ordination at the "Co(salen)" center. The oxygenation behavior of the $Co^{II}M^{II}$ complexes is studied in view of the methyl substitution on the ethylene backbone and the participation of the neighboring M^{II}. A part of this work was briefly reported previously.[9a,e]

DOI: 10.1039/b001881n

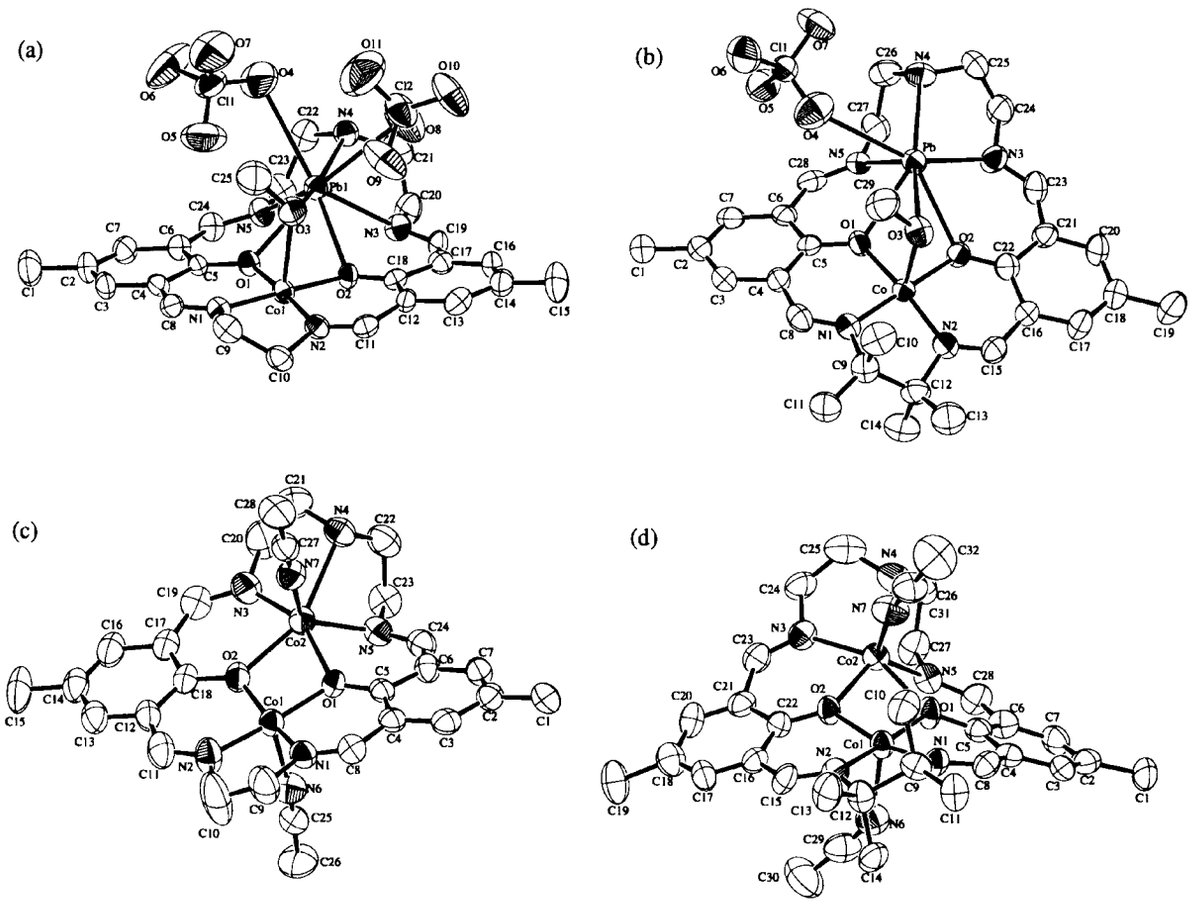

Fig. 1 Perspective views of complexes **1**·CH_3OH (a), **2**·CH_3OH (b), **3** (c), and **4** (d) with the atom numbering scheme.

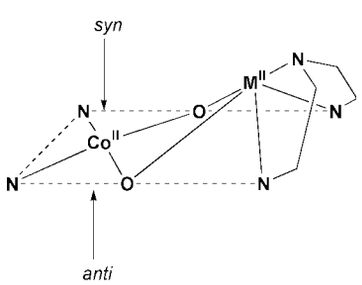

Results and discussion

Preparation

The $M^{II}Pb^{II}$ complexes of the macrocyclic ligand $(L^1)^{2-}$ can be derived by the template reaction of [*N*,*N*′-bis(3-formyl-5-methylsalicylidene)ethane-1,2-diaminato]metal(II) with diethylenetriamine (dien) in the presence of Pb^{II}.[7–11] This method was successfully applied for the synthesis of $[CoPb(L^1)(CH_3OH)][ClO_4]_2$ **1**. Similarly, $[CoPb(L^2)(CH_3OH)][ClO_4]_2$ **2**, was prepared by the reaction of *N*,*N*′-[bis(3-formyl-5-methylsalicylidene-1,1,2,2-)tetramethylethane-1,2-diaminato]cobalt(II) with dien in the presence of Pb^{II}. The FAB mass spectra of **1** and **2** exhibit a parent peak corresponding to $\{CoPb(L)(ClO_4)\}^+$ (m/z = 783 for **1** and 839 for **2**). The conversion of the CoPb complexes into the Co_2 complexes **3** and **4** was successfully achieved by transmetallation of the Pb^{II} for Co^{II}. The FAB mass spectra of **3** and **4** exhibit a parent peak corresponding to $\{Co_2(L)(ClO_4)\}^+$ (m/z = 634 for **3** and 690 for **4**).

Crystal structures of complexes 1–4

Crystal structures of complexes **1**–**4** have been determined by X-ray crystallography. Perspective views are shown in Fig. 1. The relevant bond distances and angles of the CoPb complexes (**1**·CH_3OH and **2**·CH_3OH) and the Co_2 complexes (**3** and **4**) are given in Tables 1 and 2, respectively.

The structure of complex **1**·CH_3OH was preliminarily reported.[9a] An ORTEP[14] drawing of the cationic part is given in Fig. 1(a). The Co resides in the "salen"-like N_2O_2 site and the Pb in the "saldien"-like N_3O_2 site. The Co assumes a square-pyramidal geometry with a methanol oxygen O(3) at the *syn* axial site. The basal Co–N and Co–O bond distances range from 1.871(6) to 1.901(4) Å. The axial Co–O(3) bond is longer (2.261(5) Å). The methanol oxygen attached to the *syn* axial site of the Co is weakly bonded to the Pb with the O(3)-Pb distance of 3.324(5) Å. The ethylene chain assumes the usual *gauche* conformation with a dihedral angle of 40.0°. The Pb in the N_3O_2 site has an eight-co-ordinate geometry including the methanol oxygen and two perchlorate oxygens O(4) and O(8). The exogenous Pb–O(4) (3.088(6) Å) and Pb–O(8) (2.944(6) Å) bond distances are longer than the Pb–L bond distances (2.472(5)–2.660(4) Å). The perchlorate oxygen O(4) is situated on one square face defined by O(1), O(3), N(4), and N(5) and O(8) is situated on the other face defined by O(2), O(3), N(4), and N(3). Thus, the geometry about the Pb can be regarded as a bicapped trigonal prism where one triangular face is defined by O(1), O(2), and O(3) and the other by N(3), N(4), and N(5). The Pb deviates 1.38 Å from the least-squares plane defined by O(1), O(2), N(3) and N(5) because of its large ionic radius.

An ORTEP drawing of the cationic part of complex **2**·CH_3OH is given in Fig. 1(b) together with the atom numbering scheme. The Co in the N_2O_2 site assumes a square-pyramidal geometry with the methanol oxygen O(3) at the *syn* axial site. The basal Co–N and Co–O bond distances (1.881(7)–1.926(5) Å) are comparable to those of **1**·CH_3OH and Co(salen) analogs.[15] The axial Co–O(3) bond distance is 2.222(7) Å, slightly shorter than that of **1**·CH_3OH. The methanol oxygen O(3) attached to the *syn* axial site of the Co makes a bridge to the adjacent Pb with the O(3)–Pb bond distance 3.088(8) Å.

Table 1 Selected bond distances (Å) and angles (°) of $[CoPb(L^1)(CH_3OH)][ClO_4]_2 \cdot CH_3OH$ (**1**·CH_3OH) and $[CoPb(L^2)(CH_3OH)][ClO_4]_2 \cdot CH_3OH$ (**2**·CH_3OH)

	1·CH_3OH	**2**·CH_3OH
Co–O(1)	1.895(4)	1.907(5)
Co–O(2)	1.901(4)	1.926(5)
Co–O(3)	2.261(5)	2.222(7)
Co–N(1)	1.882(5)	1.894(6)
Co–N(2)	1.871(6)	1.881(7)
Pb–O(1)	2.589(4)	2.529(5)
Pb–O(2)	2.660(4)	2.668(5)
Pb–O(3)	3.324(5)	3.088(8)
Pb–O(4)	3.088(6)	3.011(9)
Pb–O(8)	2.944(6)	
Pb–N(3)	2.528(5)	2.514(7)
Pb–N(4)	2.575(5)	2.560(7)
Pb–N(5)	2.472(5)	2.441(7)
O(1)–Co–O(2)	85.9(2)	83.3(2)
O(1)–Co–O(3)	95.0(2)	91.4(2)
O(1)–Co–N(1)	93.8(2)	94.8(2)
O(1)–Co–N(2)	173.5(2)	168.1(3)
O(2)–Co–O(3)	87.6(2)	84.8(2)
O(2)–Co–N(1)	178.0(2)	176.0(3)
O(2)–Co–N(2)	94.1(2)	96.1(3)
O(3)–Co–N(1)	94.3(2)	98.8(3)
O(3)–Co–N(2)	91.5(2)	100.3(3)
N(1)–Co–N(2)	86.0(2)	85.0(3)
O(1)–Pb–O(2)	59.0(1)	58.6(2)
O(1)–Pb–O(4)	111.1(1)	83.9(2)
O(1)–Pb–O(8)	147.3(2)	
O(1)–Pb–N(3)	110.5(1)	117.3(2)
O(1)–Pb–N(4)	140.5(2)	138.3(2)
O(1)–Pb–N(5)	70.7(2)	69.9(2)
O(2)–Pb–O(4)	155.5(1)	139.3(2)
O(2)–Pb–O(8)	96.4(2)	
O(2)–Pb–N(3)	67.3(1)	70.3(2)
O(2)–Pb–N(4)	136.3(1)	138.3(2)
O(2)–Pb–N(5)	110.6(2)	102.8(2)
O(4)–Pb–O(8)	82.0(2)	
O(4)–Pb–N(3)	134.0(2)	148.9(2)
O(4)–Pb–N(4)	66.6(2)	80.0(2)
O(4)–Pb–N(5)	83.7(2)	75.4(2)
O(8)–Pb–N(3)	73.4(2)	
O(8)–Pb–N(4)	72.1(2)	
O(8)–Pb–N(5)	141.8(2)	
N(3)–Pb–N(4)	69.0(2)	69.0(2)
N(3)–Pb–N(5)	92.2(2)	90.2(2)
N(4)–Pb–N(5)	69.8(2)	68.8(2)
Co–O(1)–Pb	100.2(2)	101.4(2)
Co–O(2)–Pb	97.6(2)	96.2(2)

The 1,1,2,2-tetramethylethylene chain assumes the usual *gauche* conformation with axial orientation of C(10) and C(14) and equatorial orientation of C(11) and C(13) with a dihedral angle of 41.8°, slightly larger than that of **1**·CH_3OH. The Pb in the N_3O_2 site has a seven-co-ordinate geometry including the methanol oxygen O(3) and a perchlorate oxygen O(4). A weak interaction exists between the Pb and the perchlorate oxygen O(8), Pb···O(8) 3.65(2) Å. Thus, the Pb in **2**·CH_3OH assumes a bicapped trigonal prism structure similar to that of **1**·CH_3OH.

The core structure of complex **2**·CH_3OH is considerably distorted compared with that of **1**·CH_3OH. The "salen"-like N_2O_2 least-squares plane and the plane defined by O(1), O(2), N(3) and N(5) are bent at the O(1)···O(2) edge with a dihedral angle of 8.83°. The corresponding dihedral angle for **1**·CH_3OH is 1.99°. Furthermore, the complex cation of **2**·CH_3OH is bent at the Co···Pb edge providing a saddle shape for the dinuclear core. The dihedral angle defined by the two aromatic rings is 21.07° (**1**·CH_3OH: 0.43°). Such a distortion in the core of **2**·CH_3OH arises from the steric repulsion between the proton attached to C(8) and the methyl group C(11) in the equatorial orientation (also repulsion between the proton attached to C(15) and the methyl group C(13): C(8)···C(11) 2.80, C(13)···C(15), 2.82 Å).

Table 2 Selected bond distances (Å) and angles (°) of $[Co_2(L^1)(CH_3CN_2)][ClO_4]_2$ **3** and $[Co_2(L^2)(CH_3CN)][ClO_4]_2$ **4**

	3	**4**
Co(1)–O(1)	1.873(5)	1.874(9)
Co(1)–O(2)	1.914(5)	1.902(10)
Co(1)–N(1)	1.875(7)	1.85(1)
Co(1)–N(2)	1.838(7)	1.85(1)
Co(1)–N(6)	2.174(9)	2.27(2)
Co(2)–O(1)	2.193(5)	2.17(1)
Co(2)–O(2)	2.163(5)	2.125(10)
Co(2)–N(3)	2.063(7)	2.08(1)
Co(2)–N(4)	2.466(7)	2.24(1)
Co(2)–N(5)	2.063(7)	2.08(1)
Co(2)–N(7)	2.074(8)	2.13(1)
O(1)–Co(1)–O(2)	82.5(2)	82.3(4)
O(1)–Co(1)–N(1)	95.3(3)	94.5(5)
O(1)–Co(1)–N(2)	175.6(3)	176.5(5)
O(1)–Co(1)–N(6)	92.4(2)	92.0(6)
O(2)–Co(1)–N(1)	167.9(3)	167.0(5)
O(2)–Co(1)–N(2)	95.8(3)	97.2(5)
O(2)–Co(1)–N(6)	94.6(3)	88.4(5)
N(1)–Co(1)–N(2)	85.5(3)	85.3(6)
N(1)–Co(1)–N(6)	97.4(3)	104.4(6)
N(2)–Co(1)–N(6)	91.7(3)	91.5(6)
O(1)–Co(2)–O(2)	70.0(2)	70.6(4)
O(1)–Co(2)–N(3)	154.4(2)	152.5(5)
O(1)–Co(2)–N(4)	130.9(2)	129.9(5)
O(1)–Co(2)–N(5)	78.9(2)	78.8(4)
O(1)–Co(2)–N(7)	84.8(2)	82.0(5)
O(2)–Co(2)–N(3)	85.6(2)	84.4(4)
O(2)–Co(2)–N(4)	155.4(2)	155.5(5)
O(2)–Co(2)–N(5)	133.0(2)	125.8(5)
O(2)–Co(2)–N(7)	92.2(2)	88.8(5)
N(3)–Co(2)–N(4)	74.7(3)	77.3(5)
N(3)–Co(2)–N(5)	115.1(3)	108.5(5)
N(3)–Co(2)–N(7)	104.1(3)	109.6(6)
N(4)–Co(2)–N(5)	70.2(2)	76.1(6)
N(4)–Co(2)–N(7)	78.8(2)	82.2(5)
N(5)–Co(2)–N(7)	119.6(3)	130.3(6)
Co(1)–O(1)–Co(2)	103.5(2)	101.7(4)
Co(1)–O(2)–Co(2)	103.3(2)	102.5(4)
Co(1)–N(6)–C(25)	172.1(9)	145(1)
Co(2)–N(7)–C(27)	175.5(7)	164(1)

A perspective view of complex **3** is shown in Fig. 1(c). The two Co are bridged by the phenolic oxygens, O(1) and O(2), with an intermetallic Co···Co separation of 3.201(2) Å. The Co(1) in the N_2O_2 site assumes a square-pyramidal geometry involving an acetonitrile nitrogen N(6) at the *anti* axial site. The basal Co–N and Co–O bond distances (1.838(7)–1.914(5) Å) are comparable to those of the precursor CoPb complex **1**·CH_3OH. The axial Co(1)–N(6) bond (2.174(9) Å) is short relative to the axial Co–O bond of **1**·CH_3OH. The Co(2) in the N_3O_2 site has a distorted six-co-ordinate geometry involving an acetonitrile nitrogen N(7). The Co(2)-to-donor bond distances are long (2.063(7)–2.466(7) Å). The acetonitrile nitrogen N(7) and the amino nitrogen N(4) are situated *cis* to each other. Interestingly, the Co(2)–N(7) bond distance (2.074(8) Å) is significantly shortened compared with Co(1)–N(6) (2.174(9) Å).

An ORTEP drawing of the cationic part of complex **4** is given in Fig. 1(d). The dinuclear core is essentially similar to that of **3**, but considerably more distorted. This distortion arises from the steric repulsion between the proton attached to C(8) and the methyl group C(11) in the equatorial orientation (also repulsion between the proton attached to C(15) and the methyl group C(13): C(8)···C(11) 2.83, C(13)···C(15) 2.92 Å) as observed for **2**·CH_3OH. The local configurations about the two Co resemble those of **3** but some geometrical changes occur. The Co(2)–N(4) bond (2.24(1) Å) is significantly short relative to that of **3**, whereas the Co(2)–N(7) (acetonitrile) bond

Table 3 Structural parameters of CoM complexes **1**·CH_3OH, **2**·CH_3OH, **3** and **4**

	1·CH_3OH	**2**·CH_3OH	**3**	**4**
Co···M/Å	3.468(1)	3.455(2)	3.201(2)	3.145(8)
d(Co)[a]/Å	0.07	0.13	0.14	0.12
d(M)[b]/Å	1.38	1.39	0.49	0.61
τ[c]/°	1.99	8.83	10.44	13.86
φ[d]/°	0.43	21.07	13.79	39.66

[a] Deviation from the least-squares plane defined by O(1), O(2), N(1) and N(2). [b] Deviation from the least-squares plane defined by O(1), O(2), N(3) and N(5). [c] The bending at the O(1)···O(2) edge between the planes defined by O(1), O(2), N(1) and N(2) and that by O(1), O(2), N(3) and N(5). [d] Dihedral angle between the two aromatic rings.

distance (2.13(1) Å) is long relative to that of **3**. A noticeable geometrical difference between **3** and **4** is seen in the axial co-ordination mode. In **3** the acetonitrile molecule co-ordinates to the Co(1) in the N_2O_2 site with a linear mode (Co(1)–N(6)–C(25), 172.1(9)°), whereas the corresponding angle (Co(1)–N(6)–C(29)) in **4** is bent (145(1)°). In addition, the axial Co–N bond distance (2.27(2) Å) for **4** is slightly elongated relative to that for **3** (2.174(9) Å). These facts can be explained by the steric repulsion between the methyl groups on the ethylene lateral chain and the axial acetonitrile molecule.

Some geometrical features in the core of the CoM complexes **1**–**4** are summarized in Table 3 for comparison. The bending at the O(1)···O(2) edge (τ) between the plane defined by O(1), O(2), N(1), and N(2) and the plane defined by O(1), O(2), N(3), and N(5) becomes larger in the order **1**·CH_3OH < **2**·CH_3OH < **3** < **4**. The bending at the Co···M edge (φ) between the two aromatic rings becomes larger in the order **1**·CH_3OH < **3** < **2**·CH_3OH < **4**. From the X-ray analyses of **1**–**4**, the change of the metal ion in the adjacent N_3O_2 site and the introduction of the methyl groups on the ethylene lateral chain give rise to a significant distortion of the macrocyclic framework.

General properties

Selected IR data are given in the Experimental section. All of the complexes show the ν(C=N) vibration at 1640–1630 cm^{-1} and the ν(NH) vibration of the secondary amine at 3280–3340 cm^{-1}. Complexes **3** and **4** show two weak bands in the region of 2280–2240 cm^{-1} that are assigned to the ν(CN) vibrations of the co-ordinated acetonitrile molecules.

The magnetic moments of complexes **1** and **2** at room temperature are 2.32 and 2.42 μ_B, respectively, which are typical of low-spin Co^{II}. Complexes **3** and **4** have a larger magnetic moment (4.61 and 4.66 μ_B per Co_2, respectively). It is evident that the Co^{II} in the N_2O_2 site is low spin whereas that in the N_3O_2 site is high spin.[7,8,9b]

The powder EPR spectrum of complex **1** was preliminarily reported;[9a] it showed a rhombic pattern with $g_x = 2.98$, $g_y = 2.20$, $g_z = 2.04$, $A_x = 113$, $A_y = 118$ and $A_z = 156$ G (gauss = 10^{-4} T). In a frozen acetonitrile at liquid nitrogen temperature **1** also shows a rhombic pattern with $g_x = 2.99$, $g_y = 2.27$, $g_z = 2.03$, and $A_z = 115$ G. Both spectra are typical of the low-spin d^7 electronic configuration with one unpaired electron in the d_{z^2} orbital.[16] EPR spectral features of **2** are very similar in the solid state and frozen acetonitrile and show a rhombic pattern of low-spin Co^{II}, though the hyperfine structures are not observed (solid, $g_x = 2.68$, $g_y = 1.86$, $g_z = 1.74$: frozen acetonitrile, $g_x = 2.49$, $g_y = 2.09$, $g_z = 2.05$). The Co_2 complexes **3** and **4** were both EPR-silent.

All of the complexes show an intense band at ≈360 nm, a shoulder at 380–420 nm, and a distinct band at ≈540 nm. The former intense band can be assigned to the π–π* transition associated with the azomethine group.[17] The last two bands with an absorption coefficient of *ca.* 1×10^3 M^{-1} cm^{-1} can be assigned to the charge-transfer bands from the filled pπ orbital of the phenolic oxygen to the vacant orbitals of Co^{II}.[9b] The molar conductances for **1**–**4** in acetonitrile fall in the range 265–274 S cm^2 mol^{-1} characteristic of 1:2 electrolytes in this solvent.[18]

Table 4 Electrochemical data of CoM complexes[a]

	Complex	$E_{1/2}$/V (ΔE/V) reduction Co^{II}–Co^{I}	oxidation Co^{II}–Co^{III}
1	CoPb(L^1)	−1.10 (0.08)	+0.20 (0.14)
2	CoPb(L^2)	−1.14 (0.13)	+0.33 (0.15)
3	Co_2(L^1)	−1.09 (0.06)	+0.27 (0.18)
4	Co_2(L^2)	−1.14 (0.08)	+0.42 (0.28)

[a] In acetonitrile (concentration 1×10^{-3} M); supporting electrolyte NEt_4ClO_4 (0.1 M); scan rate 50 mV s^{-1}; glassy-carbon working electrode; platinum auxiliary electrode; Ag–Ag^+ (NEt_4ClO_4–acetonitrile) reference electrode.

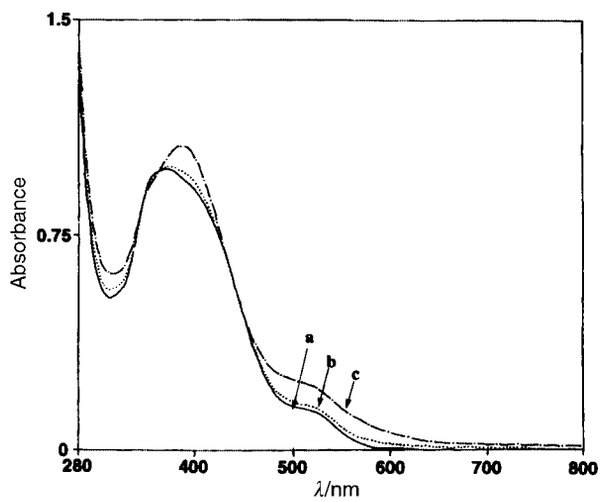

Fig. 2 Electronic spectra of complex **1** in acetonitrile (1×10^{-3} M): (a) in the absence of O_2 at 25 °C, (b) under O_2 at 25 °C, (c) under O_2 at 0 °C.

The electrochemical properties of complexes **1**–**4** were studied by cyclic voltammetry, and the numerical data are given in Table 4. All of the complexes show two quasi-reversible couples at −1.14 to −1.09 V (*vs.* Ag–Ag^+) and at +0.20–+0.42 V. They can be assigned to the Co^{I}–Co^{II} and Co^{II}–Co^{III} processes at the N_2O_2 site, respectively: the Co^{II} in the N_3O_2 site for **3** and **4** is redox-inactive due to its distorted configuration.[7,8,9b] The Co^{II}–Co^{III} couple shifts to more positive potentials on going from **1** (+0.20) to **2** (+0.33 V) and from **3** (+0.27) to **4** (+0.42 V), although it is generally known that substituent(s) introduced into the ethylene backbone of Co(salen) have only a small effect upon this couple.[19] As demonstrated by X-ray crystallography, the methyl substitution into the ethylene backbone gives rise to a large distortion in the dinuclear core of **2** and **4**. It appears that the "Co(salen)" entity is rigid and hardly adaptable to any geometrical change required for oxidation to Co^{III}. On the other hand, the methyl substitution has little effect upon the Co^{I}–Co^{II} potential because Co^{I} assumes a planar geometry.

Reactivity toward dioxygen

[CoPb(L^1)(CH_3OH)][ClO_4]$_2$ 1. The oxygenation behavior of complex **1** was examined by means of electronic and EPR spectroscopy. Introduction of dioxygen into an acetonitrile solution of **1** at 25 °C caused only a small change in the spectrum (Fig. 2(a) and (b)). When cooled to 0 °C, the solution showed an immediate change from red to dark red and exhibited an intense absorption band at 392 nm (ε 11200 M^{-1} cm^{-1}) and a broad around 560 nm (ε 1500 M^{-1} cm^{-1}) (Fig. 2(c)). The latter absorption with moderate intensity is characteristic of Co–dioxygen

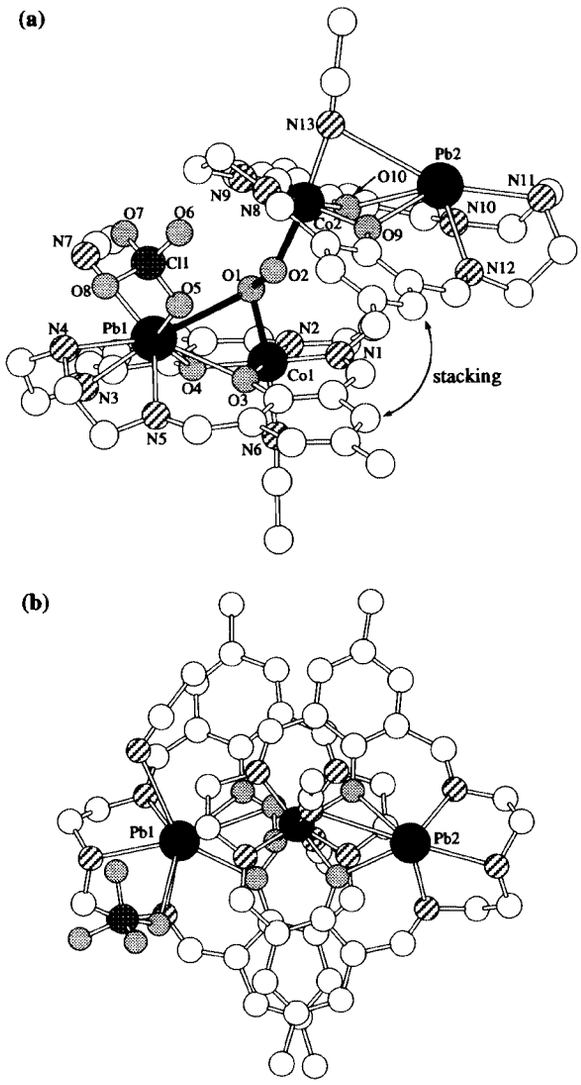

Fig. 3 Perspective views of peroxo-**1**: (a) side view, (b) top view.

complexes.[12,13] The oxygenated solution was EPR-silent. Upon warming to 25 °C, the original spectrum (Fig. 2(b)) was recovered. Thus, a reversible oxygenation/deoxygenation cycle was established for **1**.

A dioxygen adduct $[\{CoPb(L^1)(CH_3CN)\}_2(O_2)][BPh_4]_2[ClO_4]_2\cdot 4CH_3CN\cdot 5.5H_2O$ (peroxo-**1**) was isolated when an acetonitrile solution of complex **1** was oxygenated at −30 °C in the presence of an excess of $NaBPh_4$ and diffused with diethyl ether.[9e] The structure of the cationic part of peroxo-**1** is given in Fig. 3 with the atom numbering scheme. Selected bond distances and angles are given in Table 5. Since the precision of X-ray analysis for peroxo-**1** is poor owing to the limited number of reflections, detailed discussion of the bond distances and angles may not be made, but the result is useful for discussing the structural features in the solid and solution states.

The complex cation consists of one $\{CoPb(L^1)(CH_3CN)_2(ClO_4)\}$ entity (unit A), one $\{CoPb(L^1)(CH_3CN)\}$ entity (unit B) and a peroxo group. The Co(1) and Pb(1) in unit A are triply bridged by the two phenolic oxygens of $(L^1)^{2-}$ and one terminal oxygen of the peroxo group, and the Co(2) and Pb(2) in unit B are triply bridged by the two phenolic oxygens and an acetonitrile nitrogen. The intermetallic Co(1)···Pb(1) and Co(2)···Pb(2) separations are 3.460(4) and 3.452(4) Å, respectively.

The peroxo group adopts a rare μ_3-1κ*O*,2κ*O*,3κ*O*′ bridging mode, where one peroxo oxygen O(1) bridges Co(1) and Pb(1) at the *syn* site in unit A and another oxygen O(2) unidentately co-ordinates to the *anti* site of Co(2) in unit B. The O(1)–O(2) bond distance is 1.35(2) Å, which is reasonable compared with that of the μ-η¹,η¹ peroxo complexes of Co(salen) (1.383(7)–1.339(6) Å)[12e,20] but short relative to that for $[\{CoM(L^1)(AcO)\}_2(O_2)]^{2+}$ (M = Mn^{II} or Co^{II}; 1.416(5)–1.415(4) Å).[9f] The O(1)–Co(1), O(1)–Pb(1) and O(2)–Co(2) bond distances are 1.92(2), 3.12(2) and 1.88(2) Å, respectively. The Co(1)–O(1) bond distance is slightly elongated relative to Co(2)–O(2) due to the bridging function of O(1).

Table 5 Selected bond distances (Å) and angles (°) of $[\{CoPb(L^1)(CH_3CN)\}_2(O_2)][BPh_4]_2[ClO_4]_2\cdot 4CH_3CN\cdot 5.5H_2O$ (peroxo-**1**)

Co(1)···Co(2)	4.368(6)	Co(1)···Pb(1)	3.460(4)
Co(1)···Pb(2)	6.264(5)	Co(2)···Pb(1)	5.118(4)
Co(2)···Pb(2)	3.452(4)	Pb(1)···Pb(2)	8.184(2)
O(1)–O(2)	1.35(2)		
Co(1)–O(1)	1.92(2)	Co(1)–O(3)	1.94(2)
Co(1)–O(4)	1.93(2)	Co(1)–N(1)	1.86(3)
Co(1)–N(2)	1.91(2)	Co(1)–N(6)	1.93(2)
Co(2)–O(2)	1.88(2)	Co(2)–O(9)	1.91(2)
Co(2)–O(10)	1.92(2)	Co(2)–N(8)	1.84(3)
Co(2)–N(9)	1.88(2)	Co(2)–N(13)	2.08(3)
Pb(1)–O(1)	3.12(2)	Pb(1)–O(3)	2.51(2)
Pb(1)–O(4)	2.61(2)	Pb(1)–O(5)	3.09(3)
Pb(1)–N(3)	2.52(2)	Pb(1)–N(4)	2.62(3)
Pb(1)–N(5)	2.51(2)	Pb(1)–N(7)	3.06(4)
Pb(2)–O(9)	2.50(2)	Pb(2)–O(10)	2.62(2)
Pb(2)–N(10)	2.53(2)	Pb(2)–N(11)	2.57(3)
Pb(2)–N(12)	2.49(2)	Pb(2)–N(13)	3.20(2)
Co(1)–O(1)–O(2)	114(1)	Co(2)–O(2)–O(1)	117(1)
Pb(1)–O(1)–O(2)	93(1)	Co(1)–O(1)–Pb(1)	83.0(6)
Co(1)–O(3)–Pb(1)	101.1(8)	Co(1)–O(4)–Pb(1)	98.1(8)
Co(2)–O(9)–Pb(2)	102.3(8)	Co(2)–O(10)–Pb(2)	97.6(7)
Co(2)–N(13)–Pb(2)	78.6(8)		

In unit A Co(1) in the N_2O_2 site has a pseudo octahedral geometry together with the peroxo oxygen O(1) at the *syn* axial site and an acetonitrile nitrogen N(6) at the *anti* axial site. The Pb(1) in the N_3O_2 site is eight-co-ordinated including the peroxo oxygen O(1), an acetonitrile nitrogen N(7) and a perchlorate oxygen O(5). The geometry about Co(2) in unit B is also pseudo octahedral with the peroxo oxygen O(2) at the *anti* axial site and an acetonitrile nitrogen N(13) at the *syn* axial site. The acetonitrile nitrogen N(13) makes a bridge to the adjacent Pb(2) completing six-co-ordination. The Pb(2)–N(13) bridge distance is 3.20(2) Å. The Co(1)–N(6) (1.93(2) Å) and Co(2)–N(13) (2.08(3) Å) bond distances are considerably short relative to the Co–N(acetonitrile) for **3** (2.174(9) Å) and **4** (2.27(2) Å) in accord with the 3+ oxidation state of the Co in peroxo-**1**.

The acetonitrile molecule bound to Pb(1) in unit A is oriented nearly parallel to one aromatic ring with interatomic separations of 3.32–3.54 Å. Further, units A and B in a molecule are stacked at one phenolate moiety with an average ring–ring separation of 3.6 Å. This is clearly seen when the molecule is projected along the peroxo O(1)–O(2) linkage (Fig. 3(b)).

To the best of our knowledge, peroxo-**1** is the first example of a μ_3-1κ*O*,2κ*O*,3κ*O*′ peroxo-bridged complex. Evidently, the Pb^{II} in the neighboring N_3O_2 site plays an important role in the oxygenation at the "Co(salen)" center. The most preferred bridging mode in the present case must be μ_4-1κ*O*,2κ*O*,3κ*O*′, 4κ*O*′, but peroxo-**1** cannot have such a peroxo bridge because of a large steric hindrance occurring between two $\{CoPb(L^1)\}$ moieties in this bridge.

In order to gain further insight into the oxygenation behavior of complex **1** and the solution structure of peroxo-**1**, ^1H, ^{13}C NMR and ^{13}C–^1H COSY spectroscopic studies were performed. The ^1H NMR spectrum of **1** in d_3-acetonitrile (Fig. 4(a)) showed well resolved isotropically shifted resonances spread from δ −40 to +20, due to the paramagnetic nature of Co^{II}. The sharp resonance at δ 3.32 is assigned to the methyl proton of the methanol molecule liberated in solution. Twelve resonances are observed for $[CoPb(L^1)]^{2+}$, indicating that **1**

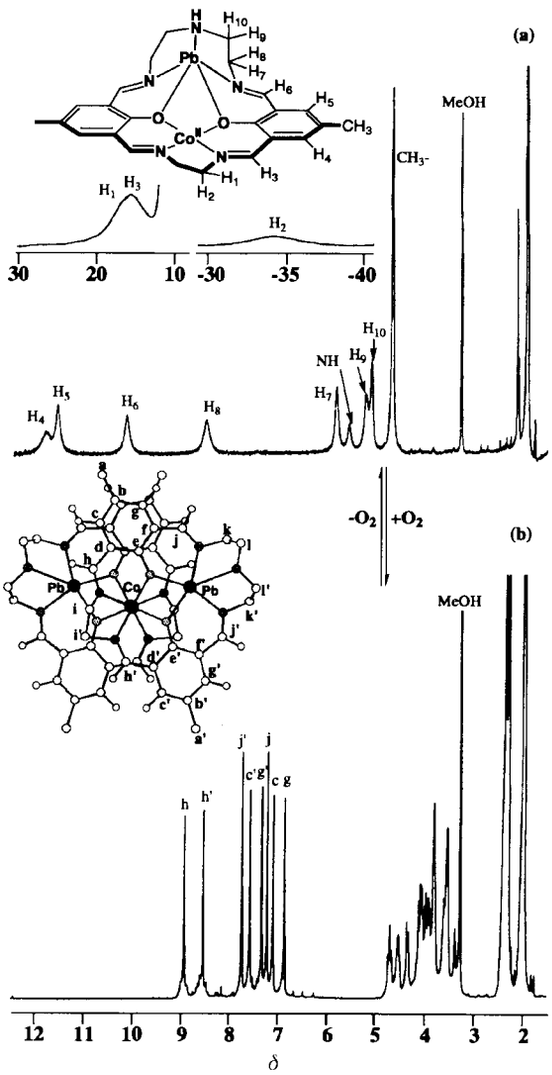

Fig. 4 ^{1}H NMR spectra of complex **1** in d_3-acetonitrile at −20 °C: (a) under Ar, (b) under O_2.

has C_s symmetry with respect to the macrocyclic ligand. The assignments of the proton resonances were carried out on the basis of their relative intensities and T_1 values (see Fig. 4(a)).

Introduction of dioxygen into the d_3-acetonitrile solution of complex **1** at −20 °C caused a dramatic change in the ^{1}H NMR spectrum to show sharp resonances in the diamagnetic region (Fig. 4(b)). The most noticeable feature is a total of eight signals in the region δ 6.8–9.0. They are classified into four singlet pairs based on ^{13}C NMR, DEPT, and ^{13}C–^{1}H COSY studies (Figs. 5 and 6): (i) δ 8.87 (h) and 8.48 (h′), (ii) 7.68 (j′) and 7.15 (j), (iii) 7.52 (c′) and 7.04 (c), (iv) 7.27 (g′) and 6.81 (g). The signals (i) and (ii) are attributed to two non-equivalent azomethine protons and (iii) and (iv) to two non-equivalent ring protons. Similarly, the methyl proton on the aromatic ring also appears as two singlets at δ 2.28 (a) and 2.29 (a′). Some resonances (δ 8.48, 7.68, 7.15, 7.27, 7.04 and 6.81) exhibit a significant upfield shift relative to that of the corresponding discrete MPb(L^1) complexes (M = Ni^{II}, Co^{III} or Zn^{II})[8,9c,11b] as found for complexes having a stacking interaction.[11b,21] This result indicates that the two {CoPb(L^1)} units in peroxo-**1** are arranged in a stacked manner as confirmed by X-ray crystallography and free rotation of the {CoPb(L^1)} units with respect to the Co–O–O–Co linkage is prohibited owing to the μ_3-1κO,2κO,3$\kappa O'$ peroxo bridge. It must be emphasized that the ^{1}H NMR spectral feature for peroxo-**1** significantly differs from that of a related peroxo dimer [{CoZn(L)(AcO)}$_2$(O$_2$)]$^{2+}$ where the two {CoZn(L)(AcO)} entities can rotate about the Co–O–O–Co linkage to show a C_s symmetric feature in ^{1}H and ^{13}C NMR spectra with

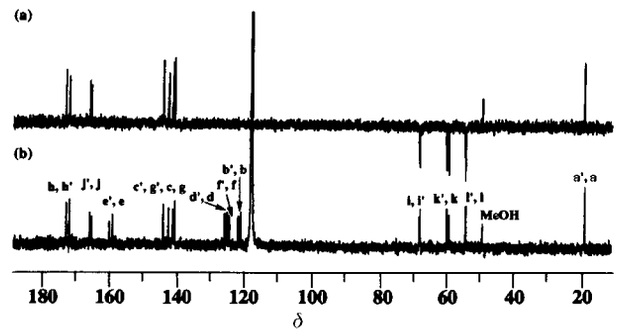

Fig. 5 DEPT (a) and ^{13}C NMR (b) spectra for peroxo-**1** measured at −20 °C in d_3-acetonitrile.

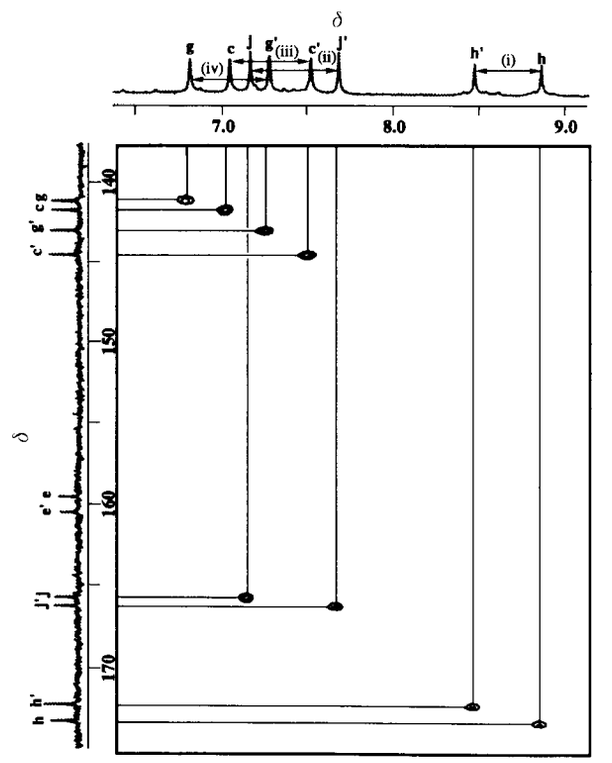

Fig. 6 ^{13}C–^{1}H COSY spectrum of peroxo-**1** measured at −20 °C in d_3-acetonitrile.

respect to the macrocyclic ligand.[22] The stacked structure of peroxo-**1** in solution is also supported by ^{13}C NMR and DEPT spectroscopy in d_3-acetonitrile (Fig. 5). It shows 24 independent carbon resonances, in addition to a resonance at δ 31.2 attributable to the methanol molecule liberated in solution.

It must be noted that there is a remarkable difference in oxygenation between Co(salen) and complex **1**; Co(salen) predominantly forms a superoxo complex in a dilute solution,[12,13] whereas a peroxo complex of Co(salen) forms in co-ordinative solvents such as dmf or pyridine at high concentration.[13g] The formation of peroxo-**1** occurs even in weak co-ordinative solvents such as acetonitrile or acetone at low concentration. Thus, the formation of peroxo-**1** is ascribed to a neighboring effect of the Pb in incorporating dioxygen. In spite of many efforts using the resonance Raman technique we were unsuccessful in determining ν(O–O), ν(Co–O), ν(Pb–O) vibrations for peroxo-**1**.

[Co$_2$(L^1)(CH$_3$CN)$_2$][ClO$_4$]$_2$ 3. Complex **3** was sensitive to dioxygen and irreversibly oxidized even at −30 °C, and the formation of a peroxo complex was not confirmed. It should be noted that there is a remarkable difference in oxygenation between **1** and **3** which differ only in the metal ion in the N_3O_2 site. Thus, the high sensitivity of **3** suggests that the Co^{II} in the adjacent N_3O_2 site is involved in the irreversible oxidation. The

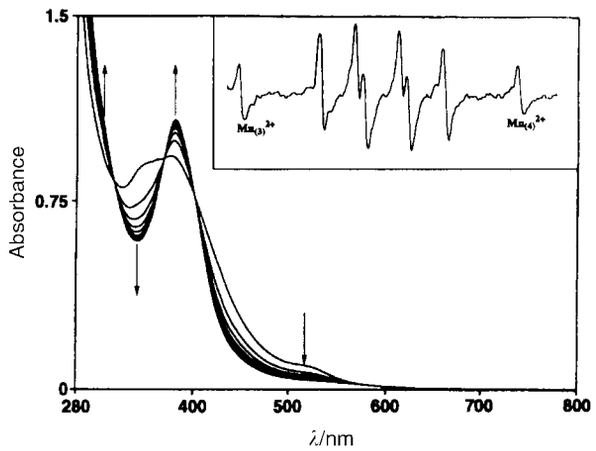

Fig. 7 Spectral changes for complex **3** under dioxygen in acetonitrile at −30 °C. The insert is the EPR spectrum for the oxygenated solution of **3** in the presence of DMPO.

spectral changes for **3** in the presence of dioxygen are shown in Fig. 7. The absorption spectrum of **3** changed with time and finally showed a distinct band at 380 nm and a moderately intense band around 520 nm. The spectral change was found to be slowed at high concentration. This reminds us that a superoxo complex and a peroxo complex exist in equilibrium upon oxygenation of Co(salen) and its analogs.[12,13] The presence of a superoxo species in the reaction of **3** with dioxygen has been supported by EPR studies using DMPO (5,5′-dimethyl-1-pyrroline *N*-oxide). The EPR signal with a four-line hyperfine structure observed ($a_\alpha^N = 13.5$, $a_\beta^H = 10.8$ G) is typical of the DMPO radical (Fig. 7, insert).[23]

As confirmed by the X-ray analysis for peroxo-**1**, oxygenation to form a superoxo complex can occur at either a *syn* or *anti* axial site of the "Co(salen)" center. If it occurs at the *syn* axial site the terminal superoxo oxygen of the resulting $[Co^{III}Co^{II}(L^1)(CH_3CN)_2(O_2^-)]^{2+}$ can make a bond to the adjacent Co^{II} in the N_3O_2 site, by kicking out one acetonitrile molecule, forming an intramolecular-type peroxo complex $[Co^{III}_2(L^1)(CH_3CN)(O_2)]^{2+}$. The final product isolated from the irreversible oxidation was found to be a $Co^{III}Co^{II}$ complex $[Co_2(L^1)(AcO)][ClO_4]_2\cdot dmf\cdot H_2O$ (oxi-**3**). It is likely that the resulting Co^{III} in the N_3O_2 site may act as a strong oxidant to oxidize intact **3** to oxi-**3**. Such irreversible oxidation has been observed for the analogous $[Co_2(L^1)(NCS)]^+$ having the same core structure.[9f] It must be mentioned that the analogous $[Co_2(L^1)(AcO)]^+$ forms a stable peroxo dimer, $[\{Co_2(L^1)(AcO)\}_2(O_2)]^{2+}$.[9f] In this case the oxygenation occurs at the *anti* axial site of the "Co(salen)" because the *syn* axial site is occupied by an acetate oxygen in a *O*,*O*′ bridging manner. Therefore, these results indicate that the reactivities of the $Co^{II}M^{II}(L^1)$ complexes toward molecular dioxygen are significantly influenced by the neighboring M^{II} in the N_3O_2 site and the core structure.

$[CoPb(L^2)(CH_3OH)][ClO_4]_2$ 2 and $[Co_2(L^2)(CH_3CN)_2][ClO_4]_2$ 4. It is known that the complex [1,1,2,2-tetramethyl-*N*,*N*′-bis(salicylidene)ethane-1,2-diaminato]cobalt(II) (Co(saltm)) reacts with dioxygen forming a superoxo complex.[12,13] On the other hand, **2** showed no reactivity toward dioxygen even at low temperature and in the presence of a Lewis base. Similarly, **4** showed no reactivity toward dioxygen. This inertness of **2** and **4** is ascribed to the methyl substituents introduced into the ethylene backbone. The structural studies for peroxo-**1** and $[\{CoM(L^1)(AcO)\}_2(O_2)]^{2+}$ indicate that the axial Co–O(peroxo) and Co–X (X = acetonitrile N for the former and acetate O in the latter) bond distances are significantly short (1.8–2.0 Å). The acyclic ligand complex Co(saltm) is flexible enough so as to accommodate a superoxo oxygen and an exogenous donor at the axial sites in such a short bond distance.[12e] On the other hand, the "Co(saltm)" entity in **2** and **4**, embedded in the macrocyclic framework, is rigid and cannot accommodate dioxygen and an exogenous ligand at the axial sites in such a short distance.

Conclusion

The $Co^{II}M^{II}$ (M = Pb or Co) complexes of the macrocycles $(L^1)^{2-}$ and $(L^2)^{2-}$ showed different oxygenation at the "Co(salen)" center, affected by the M^{II} in the adjacent N_3O_2 site and by the absence or presence of methyl substituents on the ethylene backbone. The complex $[CoPb(L^1)(CH_3OH)][ClO_4]_2$ **1** showed a reversible oxygenation in acetonitrile at 0 °C to form a peroxo complex $[\{CoPb(L^1)(CH_3CN)\}_2(O_2)]^{4+}$ (peroxo-**1**). The peroxo group assumes a rare μ_3-1κ*O*,2κ*O*,3κ*O*′ binding mode, where one peroxo oxygen bridges the Co and Pb in one $\{CoPb(L^1)(CH_3CN)\}$ unit and another oxygen is unidentate to the Co in another unit. Based on NMR spectroscopic studies for peroxo-**1**, the unusual peroxo bridge is also retained in solution, indicating that oxygenation in the *syn* axial position is facilitated by the Pb–O_2^{2-} interaction. On the other hand, $[Co_2(L^1)(CH_3CN)_2][ClO_4]_2$ **3** was very sensitive to dioxygen so as to be irreversibly oxidized even at −30 °C. This is explained by the participation of the adjacent Co^{II} in oxygenation to form an intramolecular-type peroxo complex, $[Co_2(L^1)(O_2)]^{2+}$, which is converted into a $Co^{III}Co^{II}$ complex, $[Co_2(L^1)(AcO)][ClO_4]_2\cdot dmf\cdot H_2O$ (oxi-**3**). The complexes $[CoPb(L^2)(CH_3OH)][ClO_4]_2$ **2** and $[Co_2(L^2)(CH_3CN)_2][ClO_4]_2$ **4** were inert toward dioxygen because the "Co(saltm)" entity in these complexes has little adaptability for six-co-ordination with dioxygen and an exogenous ligand in a short distance. Thus, the present study indicates that the reactivities of the $Co^{II}M^{II}$ complexes toward dioxygen at the "Co(salen)" center can be changed by the neighboring M^{II} and the methyl substituents on the ethylene backbone.

Experimental

Measurements

Elemental analyses (C, H and N) were obtained from the Service Center of Elemental Analysis at Kyushu University. Infrared spectra were recorded on a JASCO IR-810 spectrophotometer using KBr disks, electronic spectra in acetonitrile (≈1×10^{-3} M) on Shimadzu MPS-2000 and UV-3100 spectrophotometers. Magnetic susceptibilities were measured on a Faraday balance at room temperature. NMR spectra were recorded on JEOL JNM-GX 400 and EX-270 spectrometers using tetramethylsilane (TMS) as the internal standard. Molar conductance was measured in acetonitrile (≈1×10^{-3} M) on a DKK AOL-10 conductivity meter at room temperature. Fast atom bombardment (FAB) mass spectra were obtained on a JEOL JMS-SX102A/102A BE/BE four-sector type tandem mass spectrometer using 3-nitrobenzyl alcohol as the matrix. X-Band EPR spectra were recorded on a JEOL JEX-FE3X spectrometer. Cyclic voltammograms were recorded on a BAS CV-50 electrochemical analyzer in acetonitrile (≈1×10^{-3} M) containing tetraethylammonium perchlorate (≈1×10^{-1} M) as the supporting electrolyte (**CAUTION**: NEt_4ClO_4 is explosive and should be handled with great care). A three-electrode cell was used which was equipped with a glassy carbon working electrode, a platinum coil as the counter electrode, and a $Ag–Ag^+$ (NEt_4ClO_4–acetonitrile) reference electrode.

Preparations

Unless otherwise stated all chemicals were purchased from commercial sources and used without further purification. Solvents were purified and dried by standard methods. 2,6-Diformyl-4-methylphenol[24] and 1,1,2,2-tetramethylethane-1,2-diamine[25] were prepared by the literature methods. *N*,*N*′-Bis(3-formyl-5-methylsalicylidene)ethane-1,2-diamine, *N*,*N*′-bis(3-formyl-5-methylsalicylidene)-1,1,2,2-tetramethylethane-

Table 6 Crystallographic data for complexes **1**·CH_3OH, **2**·CH_3OH, **3**, **4** and peroxo-**1**

	1·CH_3OH	**2**·CH_3OH	**3**	**4**	peroxo-**1**
Formula	$C_{26}H_{35}Cl_2CoN_5O_{12}Pb$	$C_{30}H_{43}Cl_2CoN_5O_{12}Pb$	$C_{28}H_{33}Cl_2Co_2N_7O_{10}$	$C_{32}H_{41}Cl_2Co_2N_7O_{10}$	$C_{108}H_{105}B_2Cl_2Co_2N_{16}O_{19.5}Pb_2$
M	946.63	1002.74	816.38	872.49	2563.91
Crystal system	Orthorhombic	Monoclinic	Monoclinic	Hexagonal	Orthorhombic
Space group	*Pbca*	$P2_1/c$	$P2_1/c$	$P6_5$	*Pbca*
a/Å	19.985(5)	16.593(8)	10.800(2)	13.563(7)	44.812(7)
b/Å	19.711(2)	12.024(6)	36.598(5)		27.865(7)
c/Å	16.547(3)	20.068(6)	9.393(3)	35.80(2)	18.344(3)
β/°		109.72(3)	112.17(2)		
V/Å^3	6518(1)	3768(2)	3438(1)	5702(5)	22906(6)
Z	8	4	4	6	8
μ/cm^{-1}	59.09	51.15	11.85	10.77	33.38
No. reflections	6351	7098	4494	3915	14160
No. observations ($I > 3.00\ \sigma(I)$)	3737	5302	2465	2643	4731
No. variables	425	461	433	429	643
R	0.032	0.051	0.048	0.083	0.065
R_w	0.023	0.077	0.060	0.116	0.071

1,2-diamine and their mononuclear cobalt(II) complexes were obtained by the literature methods.[26] All the operations for syntheses of the complexes were carried out in an atmosphere of nitrogen using a glove-box of Vacuum Atmospheres Company, Model MO-40-IV, or in an atmosphere of argon using a standard Schlenk apparatus to avoid oxidation from atmospheric dioxygen. **CAUTION**: the perchlorate complexes described below may be explosive and should be handled with great care.

$[CoPb(L^1)(CH_3OH)][ClO_4]_2$ 1. A suspension of [*N*,*N*′-bis-(3-formyl-5-methylsalicylidene)ethane-1,2-diaminato]cobalt(II) (1.00 g, 2.4 mmol) in methanol (50 cm^3) and a solution of $Pb(ClO_4)_2$·$3H_2O$ (1.104 g, 2.4 mmol) in methanol (10 cm^3) were combined and stirred for 30 minutes at room temperature. A methanolic solution (10 cm^3) of diethylenetriamine (0.272 g, 2.4 mmol) was dropwise added in the course of 20 minutes, and the mixture refluxed for 1 h to give a red crystalline precipitate. Yield: 2.0 g (91%). Calc. for $C_{25}H_{31}Cl_2CoN_5O_{11}Pb$: C, 32.83; H, 3.42; N, 7.66%. Found: C, 32.99; H, 3.25; N, 7.82%. μ_{eff} per Co: 2.32 μ_B at 290 K. FAB MS: *m*/*z* 783 for $\{CoPb(L^1)(ClO_4)\}^+$. Selected IR data [ν/cm^{-1}] using KBr disks: 3320, 2930, 2860, 1630, 1140, 1180 and 1080. Molar conductance [Λ_M/S cm^2 mol^{-1}] in acetonitrile: 270. UV-vis data [λ/nm (ε/M^{-1} cm^{-1})] in acetonitrile: 370 (9500), 420 (sh) and 540 (1200).

A portion of complex **1** was recrystallized from methanol–2-propanol (1 : 1 in volume) to form a methanol adduct **1**·CH_3OH suitable for X-ray crystallography.

$[CoPb(L^2)(CH_3OH)][ClO_4]_2$ 2. This complex was obtained as red crystals in a way similar to that for **1** by the reaction of [*N*,*N*′-bis(3-formyl-5-methylsalicylidene)-1,1,2,2-tetramethylethane-1,2-diaminato]cobalt(II) with diethylenetriamine. Yield: 1.85 g (89%). Calc. for $C_{29}H_{39}Cl_2CoN_5O_{11}Pb$: C, 35.88; H, 4.05; N, 7.21%. Found: C, 35.82; H, 3.78; N, 7.43%. μ_{eff} per Co: 2.42 μ_B at 290 K. FAB MS: *m*/*z* 839 for $\{CoPb(L^2)(ClO_4)\}^+$. Selected IR data [ν/cm^{-1}] using KBr disks: 3280, 2960, 2910, 2850, 1620, 1640, 1140, 1115 and 1080. Molar conductance [Λ_M/S cm^2 mol^{-1}] in acetonitrile: 265. UV-vis data [λ/nm (ε/M^{-1} cm^{-1})] in acetonitrile: 366 (10 800), 420 (sh) and 520 (1100).

The complex was recrystallized from methanol–2-propanol (1 : 1 in volume) as **2**·CH_3OH suitable for X-ray crystallography.

$[Co_2(L^1)(CH_3CN)_2][ClO_4]_2$ 3. An acetonitrile solution (10 cm^3) of complex **1** (0.365 g, 0.4 mmol) and a methanol solution (2 cm^3) of $CoSO_4$·$6H_2O$ (0.104 g, 0.4 mmol) were combined, and the mixture was refluxed for 1 h and evaporated. The residue was dissolved in acetonitrile (10 cm^3), insoluble $PbSO_4$ separated by suction filtration, and the filtrate evaporated to dryness. The resulting crude product was dissolved in acetonitrile and the solution layered with 2-propanol to form red crystals. The yield was 0.23 g (85%). Calc. for $C_{28}H_{33}Cl_2Co_2N_7O_{10}$: C, 41.19; H, 4.07; N, 12.01%. Found: C, 40.93; H, 3.89; N, 11.61%. μ_{eff} per Co_2: 4.61 μ_B at 290 K. FAB MS: *m*/*z* 634 for $\{Co_2(L^1)(ClO_4)\}^+$. Selected IR data [ν/cm^{-1}] using KBr disks: 3340, 2920, 2840, 2280, 2240, 1630, 1140, 1110 and 1080. Molar conductance [Λ_M/S cm^2 mol^{-1}] in acetonitrile: 274. UV-vis data [λ/nm (ε/M^{-1} cm^{-1})] in acetonitrile: 352 (9500), 380 (sh) and 520 (1000).

$[Co_2(L^2)(CH_3CN)_2][ClO_4]_2$ 4. This complex was obtained as red crystals in a way similar to that for **3**. The yield was 0.35 g (86%). Calc. for $C_{32}H_{41}Cl_2Co_2N_7O_{10}$: C, 44.05; H, 4.74; N, 11.24%. Found: C, 44.00; H, 4.76; N, 11.20%. μ_{eff} per Co_2: 4.66 μ_B at 290 K. FAB MS: *m*/*z* 690 for $\{Co_2(L^2)(ClO_4)\}^+$. Selected IR data [ν/cm^{-1}] using KBr disks: 3330, 2960, 2920, 2850, 2270, 2240, 1630, 1145, 1100 and 1080. Molar conductance [Λ_M/S cm^2 mol^{-1}] in acetonitrile: 272. UV-vis data [λ/nm (ε/M^{-1} cm^{-1})] in acetonitrile: 352 (10 050), 410 (sh) and 520 (1000).

Oxygenated and oxidized complexes. Reactivities of complexes **1**–**4** toward dioxygen were investigated in acetonitrile. A peroxo complex of **1** (peroxo-**1**) and an oxidized complex of **3** (oxi-**3**) were isolated as described below.

*$[\{CoPb(L^1)(CH_3CN)\}_2(O_2)][BPh_4]_2[ClO_4]_2$·$4CH_3CN$·$5.5H_2O$ (peroxo-**1**).* An acetonitrile solution (20 cm^3) of **1** (0.365 g, 0.4 mmol) was diffused with diethyl ether under dioxygen at −30 °C to give a very thin dark red crystal of peroxo-**1**.

*$[Co_2(L^1)(AcO)][ClO_4]_2$·dmf·$H_2O$ (oxi-**3**).* Complex **3** (0.30 g, 0.367 mmol) was dissolved in dmf (10 cm^3) and molecular dioxygen was bubbled into the solution for 10 minutes at −30 °C. The mixture was allowed to stand for 1 day and warmed to ambient temperature. Then a dmf solution (5 cm^3) of sodium acetate (0.15 g, 1.84 mmol) was added, and the mixture layered with 2-propanol to form brown microcrystals. The yield was 0.10 g (31%). Calc. for $C_{29}H_{39}Cl_2Co_2N_6O_{14}$: C, 39.38; H, 4.44; N, 9.50%. Found: C, 39.13; H, 4.34; N, 9.85%. Selected IR data [ν/cm^{-1}] using KBr disks: 3330, 2910, 2850, 1650, 1630, 1560, 1420, 1140, 110 and 1080. μ_{eff} per Co_2: 4.20 μ_B at 290 K.

X-Ray crystallography

Single crystals of complexes **1**·CH_3OH and **2**·CH_3OH were enclosed in a capillary tube together with the mother-solution. Each single crystal of **3** and **4** was mounted on a glass fiber and coated with epoxy resin. A single crystal of peroxo-**1** was picked up on a hand-made cold copper plate mounted inside a liquid N_2 Dewar vessel and mounted on a glass rod at −80 °C. Measurements for **1**·CH_3OH, **2**·CH_3OH, and **4** were made on a

Rigaku AFC7R diffractometer with graphite monochromated Mo-Kα radiation ($\lambda = 0.71069$ Å) and a 12 kW rotating anode generator at 23 °C. The data were collected using an ω–2θ scan technique. Measurements for peroxo-**1** and **3** were made on a Rigaku RAXIS-IV imaging plate area detector using graphite monochromated Mo-Kα radiation ($\lambda = 0.710\ 70$ Å) at −120 °C for peroxo-**1** and at 23 °C for **3**. The data were corrected for Lorentz and polarization effects, but not for absorption. Crystal data are summarized in Table 6.

The structures were solved by direct methods and expanded using Fourier techniques. The non-hydrogen atoms were refined anisotropically for **1**·CH_3OH, **2**·CH_3OH, **3** and **4**. For peroxo-**1** the non-hydrogen atoms except for the metal ions and the peroxo group were refined isotropically. Hydrogen atoms were included in the structure factor calculation but not refined. Full-matrix least-squares refinements were based on observed reflections with $I > 3.00\sigma(I)$. The crystal structure of **4** could be solved by applying both the space groups $P6_1$ and $P6_5$. The final R and R_w values were almost the same. Since, in this study, we could not distinguish these two space groups, we give the results obtained by applying $P6_5$.

CCDC reference number 186/2046.

See http://www.rsc.org/suppdata/dt/b0/b001881n/ for crystallographic files in .cif format.

Acknowledgements

The authors thank Professor T. Kitagawa and Dr M. Mukai of the Institute for Molecular Science for measurement of resonance Raman spectra. This work was supported by a Grant-in-Aid for Scientific Research (No. 09440231), Scientific Research on Priority Area "Metal-assembled Complexes" (No. 10149106) and an International Scientific Research Program (No. 09044093) from the Ministry of Education, Science, and Culture, Japan and by the JSPS Research Fellowships for Young Scientists (H. F.).

References

1 Special thematic issue on *Metal–Dioxygen Complexes*, *Chem. Rev.*, 1994, **94**, 567; *Bioinorganic Enzymology*, *Chem. Rev.*, 1996, **96**, 2237.
2 *Bioinorganic Catalysis*, 2nd edn., eds. J. Reedijk and E. Bouwman, Marcel Dekker, New York, 1999; K. D. Karlin and Y. Gultneh, *Prog. Inorg. Chem.*, 1987, **35**, 219; N. Kitajima, *Adv. Inorg. Chem.*, 1992, **39**, 1; W. B. Tolman, *Acc. Chem. Rev.*, 1997, **30**, 227; S. J. Lippard, *Angew. Chem., Int. Ed. Engl.*, 1988, **27**, 344; L. Que, Jr. and A. E. True, *Prog. Inorg. Chem.*, 1990, **38**, 97; L. Que, Jr. and Y. Dong, *Acc. Chem. Rev.*, 1996, **29**, 190; A. M. Valentine and S. J. Lippard, *J. Chem. Soc., Dalton Trans.*, 1997, 3295; L. Que, Jr., *J. Chem. Soc., Dalton Trans.*, 1997, 3933.
3 N. H. Pilkington and R. Robson, *Aust. J. Chem.*, 1970, **23**, 2225; S. F. Groh, *Isr. J. Chem.*, 1976/77, **15**, 277; R. C. Long and D. N. Hendrickson, *J. Am. Chem. Soc.*, 1983, **105**, 1513; H. Ōkawa, Y. Aratake, K. Motoda, M. Ohba, H. Sakiyama and N. Matsumoto, *Supramol. Chem.*, 1996, **6**, 293; D. Luneau, J.-M. Savariault, P. Cassoux and J.-P. Tuchagues, *J. Chem. Soc., Dalton Trans.*, 1988, 1225; R. R. Gagne, C. L. Spiro, T. J. Smith, C. A. Hamann, W. R. Thies and A. K. Shiemke, *J. Am. Chem. Soc.*, 1981, **103**, 4073; S. L. Lambert, C. L. Spiro, R. R. Gagne and D. N. Hendrickson, *Inorg. Chem.*, 1982, **21**, 68.
4 B. Bosnich, *Inorg. Chem.*, 1999, **38**, 2554 and refs. therein.
5 H. Ōkawa, H. Furutachi and D. E. Fenton, *Coord. Chem. Rev.*, 1998, **174**, 51 and refs. therein.
6 D. E. Fenton and H. Ōkawa, *Chem. Ber./Recueil*, 1997, **130**, 433 and refs. therein.
7 H. Ōkawa, J. Nishio, M. Ohba, M. Tadokoro, N. Matsumoto, M. Koikawa, S. Kida and D. E. Fenton, *Inorg. Chem.*, 1993, **32**, 2949.
8 J. Nishio, H. Ōkawa, S. Ohtsuka and M. Tomono, *Inorg. Chim. Acta*, 1994, **218**, 27.
9 (*a*) J. Shimoda, H. Furutachi, M. Yonemura, M. Ohba, N. Matsumoto and H. Ōkawa, *Chem. Lett.*, 1996, 979; (*b*) H. Furutachi and H. Ōkawa, *Inorg. Chem.*, 1997, **36**, 3911; (*c*) H. Furutachi and H. Ōkawa, *Bull. Chem. Soc. Jpn.*, 1998, **71**, 671; (*d*) H. Furutachi, S. Fujinami, M. Suzuki and H. Ōkawa, *Chem. Lett.*, 1998, 779; (*e*) H. Furutachi, S. Fujinami, M. Suzuki and H. Ōkawa, *Chem. Lett.*, 1999, 763; (*f*) H. Furutachi, S. Fujinami, M. Suzuki and H. Ōkawa, *J. Chem. Soc., Dalton Trans.*, 1999, 2197.
10 H. Furutachi, A. Ishida, H. Miyasaka, M. Ohba, N. Fukita, H. Ōkawa and M. Koikawa, *J. Chem. Soc., Dalton Trans.*, 1999, 367.
11 M. Yamami, H. Furutachi, T. Yokoyama and H. Ōkawa, (*a*) *Chem. Lett.*, 1998, 211; (*b*) *Inorg. Chem.*, 1998, **37**, 6832.
12 (*a*) R. D. Jones, D. A. Summerville and F. Basolo, *Chem. Rev.*, 1979, **79**, 139; (*b*) C. Floriani and F. Calderazzo, *Coord. Chem. Rev.*, 1972, **8**, 57; (*c*) T. D. Smith and J. R. Pilbow, *Coord. Chem. Rev.*, 1981, **39**, 295; (*d*) G. McLendon and A. E. Martell, *Coord. Chem. Rev.*, 1976, **19**, 1; (*e*) E. C. Niederhoffer, J. H. Timmons and A. E. Martell, *Chem. Rev.*, 1984, **84**, 137.
13 (*a*) T. Tsumaki, *Bull. Chem. Soc. Jpn.*, 1938, **13**, 252; (*b*) D. Chen and A. E. Martell, *Inorg. Chem.*, 1987, **26**, 1026; (*c*) D. Chen, A. E. Martell and Y. Sun, *Inorg. Chem.*, 1989, **28**, 2647; (*d*) K. Nakamoto, Y. Nonaka, T. Ishiguro, M. W. Urban, M. Suzuki, M. Kozuka, Y. Nishida and S. Kida, *J. Am. Chem. Soc.*, 1982, **104**, 3386; (*e*) W. Kanda, H. Ōkawa, S. Kida, J. Goral and K. Nakamoto, *Inorg. Chim. Acta*, 1988, **146**, 193; (*f*) E. Ochiai, *J. Inorg. Nucl. Chem.*, 1973, **35**, 1727; (*g*) C. Floriani and F. Calderazzo, *J. Chem. Soc. A*, 1969, 946.
14 C. K. Johnson, ORTEP II, Report ORNL-5138, Oak Ridge National Laboratory, Oak Ridge, TN, 1976.
15 S. Bruckner, M. Calligaris, G. Nardin and L. Randaccio, *Acta Crystallogr., Sect. B*, 1969, **25**, 1671; R. D. Iasi, B. Post and S. L. Holt, *Inorg. Chem.*, 1971, **10**, 1498; W. P. Schaefer and R. E. Marsh, *Acta Crystallogr., Sect. B*, 1969, **25**, 1675; M. Calligaris, D. Minichelli, G. Nardin and L. Randaccio, *J. Chem. Soc. A*, 1970, 2411.
16 Y. Nishida and S. Kida, *Coord. Chem. Rev.*, 1979, **27**, 275.
17 B. Bosnich, *J. Am. Chem. Soc.*, 1968, **90**, 627.
18 W. J. Geary, *Coord. Chem. Rev.*, 1971, **7**, 81.
19 M. Hirotsu, M. Kojima, K. Nakajima, S. Kashino and Y. Yoshikawa, *Bull. Chem. Soc. Jpn.*, 1996, **69**, 2549.
20 M. Calligaris, G. Nardin and L. Randaccio, *Chem. Commun.*, 1969, 763; M. Calligaris, G. Nardin, L. Randaccio and A. Ripamonti, *J. Chem. Soc. A*, 1970, 1069; A. Audeef and W. P. Schaefer, *Inorg. Chem.*, 1976, **15**, 1432.
21 M. Shionoya, T. Ikeda, E. Kimura and M. Shiro, *J. Am. Chem. Soc.*, 1994, **116**, 3848; E. Asato, H. Furutachi, T. Kawahashi and M. Mikuriya, *J. Chem. Soc., Dalton Trans.*, 1995, 3897.
22 S. Kita, H. Furutachi and H. Ōkawa, *Inorg. Chem.*, 1999, **38**, 4038.
23 D. E. Hamilton, R. S. Drago and J. Telser, *J. Am. Chem. Soc.*, 1984, **106**, 5353.
24 D. A. Denton and H. Suschitzky, *J. Chem. Soc.*, 1963, 4741.
25 L. W. Seigle and H. B. Hass, *J. Org. Chem.*, 1940, **5**, 101; R. Sayre, *J. Am. Chem. Soc.*, 1955, **77**, 6690.
26 H. Ōkawa and S. Kida, *Inorg. Nucl. Chem. Lett.*, 1971, **7**, 751; *Bull. Chem. Soc. Jpn.*, 1972, **45**, 1759.